Renewable and Sustainable Energy Transition 2 (2022) 100037

Contents lists available at ScienceDirect

Renewable and Sustainable Energy Transition

journal homepage: www.journals.elsevier.com/renewable-and-sustainable-energy-transition

Spatially resolved generation profiles for onshore and offshore wind turbines: A case study of four Dutch energy transition scenarios

N.S. Nortier [a,*], K. Löwenthal [b], S.L. Luxembourg [c], A. van der Neut [b], A.A. Mewe [c], W.G.J.H. M. van Sark [a,**]

[a] Copernicus Institute of Sustainable Development, Utrecht University, Princetonlaan 8a, Utrecht 3584 CB, the Netherlands
[b] Geodan Amsterdam, President Kennedylaan 1, Amsterdam 1079 MB, the Netherlands
[c] TNO Energy Transition, P.O. Box 15, Petten 1755 ZG, the Netherlands

ARTICLE INFO

Keywords:
Wind energy
Wind turbine
Electricity
Supply
Generation
Profile
Pathway
Scenario
GIS
Model
Netherlands

ABSTRACT

In line with the Dutch Climate Agreement, multiple energy transition scenarios have been constructed for 2030 and 2050. To various extents, they project a shift towards decentralized and intermittent renewable electricity generation (wind and solar) and widespread deployment of electric vehicles and heat pumps. These developments impose challenges regarding electricity supply-demand mismatch and grid congestion. In order to gain an understanding of when and where such problems are likely to occur, temporally and spatially resolved interpretations of the energy transition scenarios are required. This paper focuses on Dutch wind energy supply and shows construction of geodatabases of scenario-specific, hourly onshore and offshore wind electricity generation profiles on an individual turbine level. For the geographical distribution of turbine capacity, datasets on historically operational turbines, planned wind parks and suggested future turbine distributions are utilized. Turbine electricity generation profiles are constructed using a high resolution 3D meteorological dataset and power curves of commercially available turbine models. They are corrected for air pressure deviations and a multitude of loss factors, including wake effects. Compared to the present-day situation, yearly country-level electricity generation is projected to be a factor 16.6, 24.6 or 12.8 higher in 2050 when following the Regional, National or International Steering scenarios, respectively. In comparison to both the present-day and 2030 situation, onshore electricity generation is projected to be more evenly spread over different parts of the country in 2050. All offshore wind exploration areas considered in this research are projected to be completely utilized by 2050.

1. Introduction

There is a growing international consensus on the need to mitigate global climate change. This was illustrated when parties to the United Nations framework Convention on Climate Change (UNFCCC) signed the Paris Agreement, pledging to commit to an increase in mean surface temperature (MST) well below 2 °C compared to pre-industrial levels. Moreover, the convention is 'urging efforts to limit the increase to 1.5 °C' [1]. While a rulebook for implementing the Paris Agreement has yet to be finalized, the MST target has remained unchanged up until today [2]. Environmental concerns that form the basis of the international agreement are well-founded scientifically. In their fifth assessment report, the International Panel on Climate Change (IPCC) estimates an MST increase of 3.7 °C to 4.8 °C in a worst case scenario. This overshoot of the 2 °C limit would result in extensive problems related to sea level rise, more extreme weather events, melting glaciers and ice caps, acidification of oceans and rapid shifts in ecological regions. Most

Abbreviations: ASM2, Advanced Scenario Management 2; CDF, Cumulative Distribution Function; CF, Capacity Factor; DF, Discrepancy Factor; DFC, Combined Discrepancy Factor; ETM, Energy Transition Model; GHG, Green House Gas; IEC, International Electrotechnical Commission; IPCC, International Panel on Climate Change; KNMI, Royal Netherlands Meteorological Institute; LCOE, Levelized Cost of Energy; LTA, Long-Term Average; MST, Mean Surface Temperature; PSF, Power Scaling Factor; SDE, Stimulation of Sustainable Energy Production; UNFCCC, United Nations Framework Convention on Climate Change; WEM, Wind Electricity Module.

* Corresponding author.
** Principal corresponding author.
E-mail addresses: n.s.nortier@uu.nl (N.S. Nortier), w.g.j.h.m.vansark@uu.nl (W.G.J.H.M. van Sark).

https://doi.org/10.1016/j.rset.2022.100037
Received 22 December 2021; Received in revised form 26 September 2022; Accepted 26 September 2022
Available online 3 October 2022
2667-095X/© 2022 The Authors. Published by Elsevier Ltd. This is an open access article under the CC BY license (http://creativecommons.org/licenses/by/4.0/).

Nomenclature

Symbols

U	Wind speed (m/s)
h	Height (m)
T	Temperature (K)
ρ	Air density (kg/m^3)
p	Air pressure (Pa)
P	Power (W)
N	Number of (–)
D	Rotor diameter (m)
E	Electricity output (J)

of these aspects of climate change will persist for many centuries, and thus have an irreversible character [3]. Considering mitigated scenarios, a complementary IPCC report concludes that climate change related problems are projected to be considerably lower overall when global warming is limited to 1.5 °C rather than 2 °C [4].

In line with the Paris Agreement, the Dutch Climate Agreement is formulated. It states the ambition to reduce national greenhouse gas (GHG) emissions with 49% by 2030 (compared to 1990 levels) and envisions net carbon neutrality by 2050 [5]. Based on this national agreement, various Dutch energy transition scenarios have been constructed for 2030 and 2050. These scenarios provide country-level, year-total supply and demand values for a multitude of electricity assets. To various extents, they project a shift from centralized and steerable traditional electricity generation to more decentralized and intermittent renewable electricity generation from wind turbines and solar panels. At the same time, electric vehicles and heat pumps are projected to become increasingly more widespread (see Section 2.1 for details). While contributing towards a carbon neutral energy system, these transitions are expected to impose challenges regarding electricity supply-demand mismatch and grid congestion [6–9]. In order to gain insight into when and where such problems are likely to occur, spatially and temporally resolved interpretations of the energy transition scenarios are required [10,11].

In this line of thinking, a consortium between Utrecht University, TNO Energy Transition and Geodan Amsterdam developed the Advanced Scenario Management 2 (ASM2) model. It consists of a number of supply and demand modules (wind turbines, photovoltaic (PV) solar systems, electric vehicles, heat pumps, residences, commercial buildings and industry) each capable of constructing scenario-specific low voltage (neighborhood level), mid voltage (municipality level) and high voltage (country level) electricity supply and demand profiles. Together, they allow for the construction of residual demand profiles on multiple voltage levels and the calculation of regional system performance indicators such as self-consumption, self-sufficiency and grid congestion [12]. Where Quintel's Energy Transition Model (ETM) [13] offers unparalleled scenario customization options, the ASM2 model sets itself apart from other Dutch models in terms of geographical resolution, making it suitable for national as well as regional analysis. The constructed profiles are open access and can be viewed via the interactive ASM2 Energy Transition Viewer [14] or downloaded via the ASM2 Energy Transition API [15].

Since wind electricity generation is expected to play an important role in the energy transition [16–18], it should be modeled in a technologically detailed way. The main objective of the present paper is to construct spatially resolved generation profiles for future onshore and offshore wind turbines in the Netherlands, which can be used to identify potential congestion related problems in a carbon neutral Dutch energy system. For this, a wind electricity module (WEM) is developed that is incorporated in the ASM2 model. During the construction of this module, the following research question remains central:

What are the projected regional developments in temporally resolved wind electricity generation in the Netherlands during the first half of the 21st century?

This main research question is supported by two sub questions:

1. *What are the projected regional developments in onshore and offshore wind turbine capacity?*
2. *What is the temporally resolved electricity generation of this wind turbine capacity under typical meteorological circumstances?*

Module runs are made for the present-day situation (2019), a near future scenario (2030) in line with the Dutch Climate Agreement and three distant future scenarios (2050) that differ from each other regarding the degree of decentralization of electricity generation and consumption (see Section 2.1 for details). With respect to meteorological input, the year 2017 is assumed for all runs since it can be considered typical (see Section 3.2). The main research boundaries are set by the encompassing ASM2 model. This implies a 1 h temporal resolution and a municipality level spatial resolution. However, since wind resource has a high spatial variability, generation profiles are initially calculated on turbine level. Since the focus of the ASM2 model is on assessing the performance of the energy system in terms of electricity flows (i.a. self-sufficiency and grid congestion), an extensive economical and environmental analysis is outside the scope of the present paper. And while it is not detailed how much GHG emission is avoided due to the deployment wind turbines specifically, the use of climate neutral energy transition scenarios in this study safeguards net zero GHG emission for the energy system as a whole.

Regarding the spatial planning of future wind turbine capacity, case studies have been performed by other research teams for various onshore [19,20] and offshore [21,22] regions around the world. These studies typically involve the use of wind potential and restriction maps combined with a multi-criteria or levelized cost of energy (LCOE) analysis. To the authors knowledge, no (publicly available) spatiotemporal interpretations of Dutch energy transition scenarios have been performed before. For example, while the ETM [13] does provide temporally resolved onshore and offshore wind electricity generation, it does so on a country level. Featuring an additional spatial component makes the WEM especially suitable for providing grid congestion analysis input, as the phenomenon is strongly related to both the timing and

Table 1
Country-level capacity (GWp) per category for each energy transition scenario. See text for explanations.

Scenario	Wind onshore	Wind offshore	PV small	PV large
2030 Climate Agreement	6.0	11.4	8.8	17.9
2050 Regional Steering	20.0	31.0	60.1	66.4
2050 National Steering	20.0	51.5	50.7	56.9
2050 International Steering	10.0	27.5	18.1	34.5

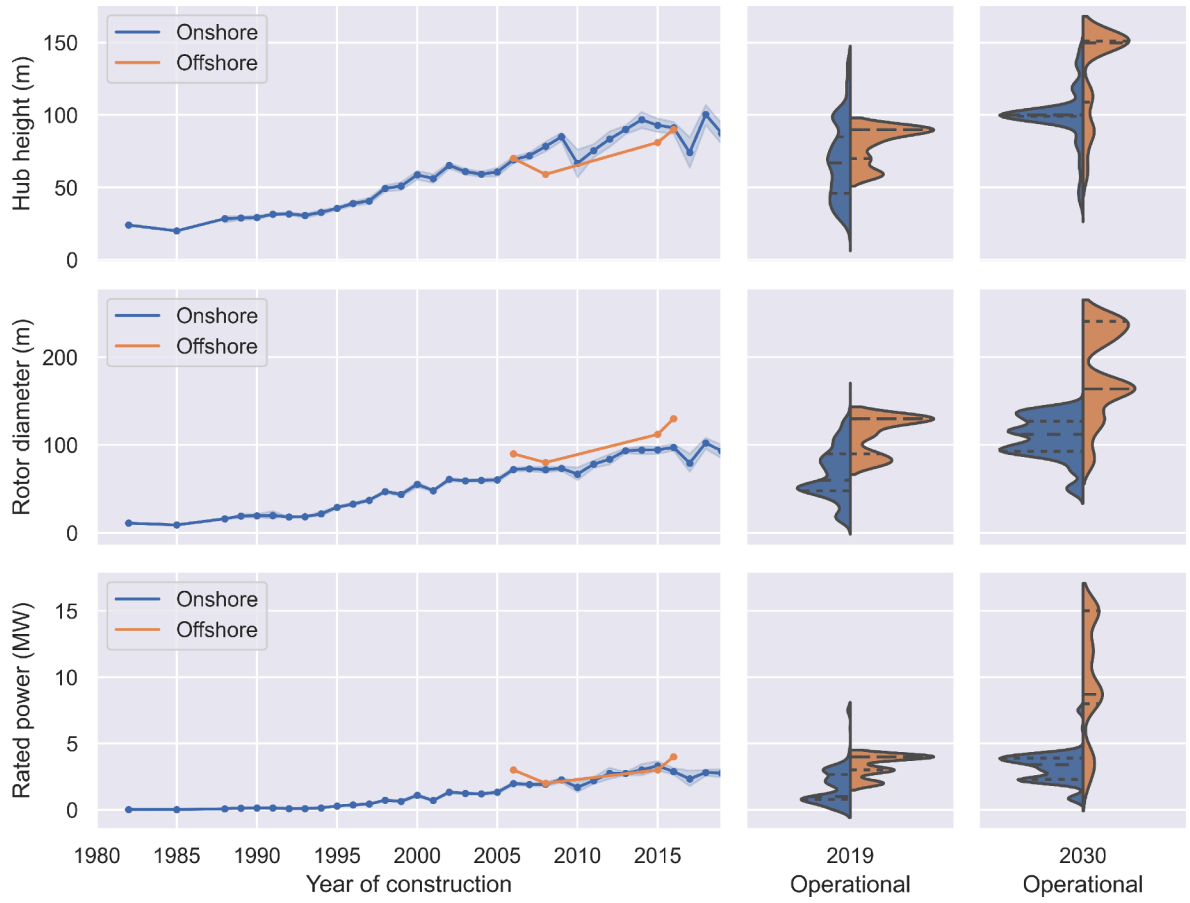

Fig. 1. Historical development of average hub height, rotor diameter and rated power for both onshore and offshore turbines constructed in the Netherlands since 1982. The violin plots show operational distributions for 2019 (present-day) and 2030 (Climate agreement scenario).

location of electricity supply and demand.

2. Methodology

2.1. Energy transition scenarios

Central to this research are four energy transition scenarios, one for 2030 and three for 2050. This section describes their implications for the future development of wind and solar electricity in the Netherlands. The scenarios ultimately provide country-level capacity values for onshore and offshore wind turbines and small scale ($<$ 15 kWp) and large scale ($\geq$ 15 kWp) PV installations. These values are summarized in Table 1.

2.1.1. Near future (2030)

The energy transition scenario for 2030 is defined in line with the Dutch Climate Agreement, which states the ambition to scale-up the electricity generation from wind turbines and large scale PV installations to 84 TWh/yr by 2030. Offshore wind turbines should provide 49 TWh/yr of this [5]. According to the Offshore Wind Energy Roadmap 2030, that translates to a total offshore wind capacity of 11.4 GWp [23,24]. Regarding the remaining 35 TWh/yr, an elaboration on the draft Climate Agreement by Kalavasta is followed. Here, it is accounted for by a combination of 6.0 GWp onshore wind and 17.9 GWp large scale PV [25]. In addition, the Climate Agreement states an approximate 7 TWh/yr of electricity produced by small-scale PV installations [5], which Kalavasta translates to a capacity of 8.8 GWp [25].

2.1.2. Distant future (2050)

Three existing energy transition scenarios for 2050 are adopted from the study Klimaatneutrale Energiescenario's 2050 [26], which is part of the Integrale Infrastructuurverkenning 2030–2050 [17]. In this collaboration between grid operators, energy companies, industry and the Ministry of Economic Affairs and Climate Policy, the scenarios are used to assess the flexibility and infrastructural requirements under integration of large amounts of variable renewable energy sources. The scenarios sketch different carbon neutral futures based on alternative governance structures. They incorporate multiple energy carriers (electricity, heat, biogas and hydrogen) and warrant that their demand is met at any moment in time, which safeguards the sensibility of the wind and PV capacity projections. The following paragraphs summarize the narratives of the three scenarios adopted for this research: Regional Steering (regionale sturing), National Steering (nationale sturing) and International Steering (internationale sturing).

In the Regional Steering scenario, local and regional authorities largely steer the energy transition. While a self-sufficient energy system is pursued at country level, the regional potential is fully exploited. The largely local steering accommodates close involvement of companies and citizens. This scenario shows the largest share of decentralized electricity generation, mainly due to a very high deployment of small and large scale PV (60.1 GWp and 66.4 GWp respectively). The projected onshore wind capacity is high (20.0 GWp) and the offshore wind capacity is intermediate (31.0 GWp). Geothermal district heating networks and heat pumps are the main providers of heat to buildings. Biogas and green hydrogen are utilized to meet peak electricity demands. Biogas is produced from local biomass and green hydrogen through electrolysis (using surplus wind and PV electricity) [26].

In the National Steering scenario, national authorities largely steer the energy transition. Again, a self-sufficient energy system is pursued at country level. More than in the Regional Steering scenario however, the emphasis is on the realization of very large scale projects. This is

Table 2
Annual average wind speed and extreme 50-year gust ranges per IEC wind class, at hub height. From [32].

IEC wind class	Annual average wind speed (m/s)	Extreme 50-year gust (m/s)
I	8.5–10.0	59.5–70.0
II	7.5–8.5	52.5–59.5
III	6.0–7.5	42.0–52.2
IV	0.0–6.0	0.0–42.0

reflected by the much higher deployment of offshore wind turbines (51.5 GWp) and the somewhat lower deployment of small and large scale PV (50.7 GWp and 56.9 GWp respectively). The projected onshore wind capacity is equal to that of the Regional Steering scenario (20.0 GWp). In total, the electricity generation from variable renewable resources (solar and wind) is highest in the National Steering scenario. Heat pumps and geothermal district heating networks are again the main providers of building heat. In addition to being utilized to meet peak electricity demands, biogas and green hydrogen are also directly consumed for industrial processes in this scenario. This in turn requires larger amounts of wind and PV electricity to be consumed in hydrogen electrolysis plants [26].

In the International Steering scenario, there is a strong international climate policy and an open, global market. Instead of pursuing a self-sufficient energy system at country level, energy carriers are produced where the techno-economical conditions are favorable. An advanced European infrastructure is realized to enable cross-border exchange of electricity, hydrogen, biomass and biofuel. In this scenario, the Netherlands shows a lower degree of electrification and imports large amounts of hydrogen. This allows for relatively low national capacities of onshore wind (10.0 GWp), offshore wind (27.5 GWp), small-scale PV (18.1 GWp) and large-scale PV (34.5 GWp). Hybrid hydrogen heat pumps are the main providers of building heat and green hydrogen is directly consumed for industrial processes [26].

2.2. Construction of turbine maps

This subsection covers the preparation of onshore and offshore wind turbine maps for the present-day situation and four Dutch energy transition scenarios towards 2030 and 2050. In order to be able to calculate turbine electricity supply later on (see Section 2.3), each turbine is assigned a location, rated power, hub height and power curve. The latter is selected from a combined dataset containing detailed information on 778 turbine models that are or have been commercially available [27,28].

2.2.1. Present-day

For the present-day situation (2019), the WindStats dataset [29] is used. This dataset contains a record of all turbines (once) operational in the Netherlands, including specifications such as: location, rated power, rotor diameter, hub height, model name, commission date and decommission date. Fig. 1 shows the development of hub height, rotor diameter and rated power for both onshore and offshore turbines, as available in the dataset. All turbines with a commission date later than, or a decommission date earlier than July 1st 2019 are filtered out. Then, a power curve is assigned to each of the remaining turbines through model name matching. If no exact match is found, the power curve belonging to the commercially available turbine model that shows the lowest combined discrepancy factor (DFC) for rated power and rotor diameter is appointed [27,28]:

$$DFC_{turbine\ model} = \left|\frac{P_{rated,\ turbine\ model} - P_{rated,\ turbine}}{P_{rated,\ turbine}}\right| + \left|\frac{D_{turbine\ model} - D_{turbine}}{D_{turbine}}\right| \quad (1)$$

where P_{rated} stands for rated capacity and D for rotor diameter. Subsequently an additional attribute, the power scaling factor (PSF), is assigned to be able to account for the discrepancy in rated power later on:

$$PSF_{turbine} = \frac{P_{rated,\ turbine}}{P_{rated,\ assigned\ turbine\ model}} \quad (2)$$

2.2.2. Onshore 2030

Considering the 2030 onshore situation, a portion of the present-day turbines will have been decommissioned. Assuming an average lifetime of 20 years, all turbines with a decommission date before July 1st 2030 are filtered out. Regarding wind parks that are already planned but not yet realized, a dataset containing all Stimulation of Sustainable Energy Production (SDE+) projects is consulted [30]. For the planned onshore wind parks in this dataset, the total rated power and location (town) are known. They are placed on the map at the centroids of corresponding town polygons [31]. The number of turbines in a park and their rated power are determined by:

$$N_{turbines\ in\ park} = \left\lceil \frac{P_{rated,\ park}}{P_{rated,\ target}} \right\rceil \quad (3)$$

$$P_{rated,\ turbine} = \frac{P_{rated,\ park}}{N_{turbines\ in\ park}} \quad (4)$$

where the target rated power ($P_{rated,\ target}$) is the rated power assumed to be typical for onshore turbines build in the future: 4.2 MW (educated guess, see Fig. 1). Note the ceiling operator in Eq. (3), which rounds up the number of turbines to the nearest integer. Each turbine is assigned an International Electronical Commission (IEC) wind class, which indicates the hub height wind regime the turbine is designed and optimized for [32] (see Table 2). For this, a 100 m average annual wind speed map [33] is converted to an IEC class map and spatially joined with the turbines. Since the average annual wind speed map (and therefor the IEC class map) is only available for this altitude, the turbines are also attributed a hub height of 100 m (to coincide with their assigned IEC class). Subsequently, the turbines are assigned the power curve belonging to the commercially available turbine model that shows the lowest discrepancy factor (DF) for rated power, whilst respecting their IEC class [27,28]:

$$DF_{turbine\ model} = \left|\frac{P_{rated,\ turbine\ model} - P_{rated,\ turbine}}{P_{rated,\ turbine}}\right| \quad (5)$$

In order to avoid assigning considerably outdated power curves to future turbines, models with a market launch date before January 1st 2010 are excluded. Power scaling factors are again determined using Eq. (2). In case the combined rated power of the still standing present-day and SDE+ turbines does not meet the scenario specific national total, additional wind parks are positioned at the centroids of municipality polygons [34]. This is done proportional to the already assigned rated power within each municipality. The methodology to determine the number of turbines, their hub heights, rated powers, power curve and powers scaling factors is identical between the SDE+ and additional municipality parks.

2.2.3. Offshore 2030

For the construction of the 2030 offshore map, layouts suggested by BLIX Consultancy [35] for planned but not yet realized parks in offshore wind exploration areas are selected and manually georeferenced (see Fig. A.1 for an overview of the wind exploration areas considered in this research). For park Hollandse Kust West, a variant consisting of 126 turbines (12 MW rated power, 150 m hub height, 220 m rotor diameter) spaced at 6.5D (meaning an inter-turbine distance of 6.5 times rotor diameter, so 1.43 km) is chosen. This balanced spacing results in limited wake effect related losses while leaving considerable room to expand the park with additional turbines later on. 63 similar turbines, spaced at 4.5D (0.99 km), are used to fill Park Waddenzee Noord. While involving

Table 3
Turbine loss factor ranges per category (in percentages). From [46].

Loss category	Loss factor low	Loss factor high	Loss factor applied
Downtime	2.00	3.00	2.50
Operational electrical efficiency	1.00	3.00	2.00
Turbine electricity consumption	0.50	2.00	1.25
Blade contamination and degradation	0.50	0.50	0.50
Shutdown due to adverse weather	0.50	1.00	0.75
Shutdown due to temperature	0.25	1.00	0.63
Cut-out recovery	0.30	4.00	2.15
Combined	*4.95*	*13.68*	*9.39*

considerable wake effect related losses, this narrow spacing ultimately maximizes the park's generation density. Park Ijmuiden Ver comprises 267 turbines (15 MW rated power, 151 m hub height, 241 m rotor diameter) with a balanced 6.2D (1.49 km) spacing. If the combined rated power of these planned parks and still standing present-day parks does not meet the scenario specific national offshore total, additional turbines (15 MW rated power, 151 m hub height, 241 m rotor diameter) are placed in wind exploration areas that do not have officially suggested layouts yet [36]. They are placed at centroids of a hexagonal grid with a horizontal spacing of 6.1D (1.47 km), following the medium configuration of Bulder et al. [37]. In contrast, when the scenario specific offshore rated power is lower than that of the planned and still standing parks, turbines are removed from park Ijmuiden Ver until the scenario requirement is met. The distribution of hub heights, rotor diameters and rated power are shown in Fig. 1.

2.2.4. Onshore 2050

Locations of onshore turbines operational in each 2050 scenario are adopted from one map published in the book *Energie en Ruimte* [38]. Provided in CAD format as a set of points surrounded by an outline of the Netherlands, these locations are georeferenced using control points to match the CAD outline with that of an existing shapefile of the Netherlands. The map depicts a possible image of the future, where 2254 turbines are fitted into a variety of landscape types, each characterized by specific aesthetical and configurational preferences. Since the map does not provide further turbine specifications (other than location), the scenario specific rated capacity of each of the 2254 adopted turbines is calculated by:

$$P_{rated,\,turbine} = \frac{P_{rated,\,country,\,scenario}}{N_{turbines\ in\ country}} \tag{6}$$

Subsequently, hub heights, rotor diameters, power curves and power scaling factors are calculated and assigned in the same way as is done for the onshore SDE+ and municipality turbines in the 2030 onshore situation (see Section 2.2.2).

2.2.5. Offshore 2050

Contrary to present-day offshore turbines, those that are constructed during the coming decade are assumed to still be operational in 2050. In addition, all offshore wind exploration areas [36] and freed-up locations are completely filled up with 15 MW turbines (150 m hub height, 220 m rotor diameter) following the hexagonal configuration mentioned in Section 2.2.3. In order to meet the scenario specific national total offshore rated capacity for 2050, supplementary 15 MW turbines are placed in an arbitrarily chosen area, approximately 40 km north-west of the Frisian island Vlieland.

2.3. Calculation of turbine electricity supply

Hourly electricity supply profiles are generated for each mapped turbine using the Python library WindPowerLib, which requires location specific meteorological data and various turbine specifications to operate [39]. The Royal Netherlands Meteorological Institute (KNMI) provides hourly, 3 dimensional meteorological time series with a horizontal resolution of 2.5 km and an irregular vertical interval. They are reconstructed from historical measurements using the currently operational meteorological model HARMONIE [40]. Wind speed, air temperature and air pressure data are extracted for the turbine location. WindPowerLib then converts these to hub height values. For wind speed, this is done using logarithmic interpolation between the closest available lower and higher altitude data points:

$$U_{hub} = U_{lower} + \left(U_{higher} - U_{lower}\right)\cdot\frac{\ln h_{hub} - \ln h_{lower}}{\ln h_{higher} - \ln h_{lower}} \tag{7}$$

where U is wind speed (m/s) and h is height (m). Air temperature is converted to hub height using linear interpolation between the closest available lower and higher altitude data points:

$$T_{hub} = T_{lower} + (h_{hub} - h_{lower})\cdot\frac{T_{higher} - T_{lower}}{h_{higher} - h_{lower}} \tag{8}$$

where T is temperature (K). Finally, hub height air density is calculated from air pressure at the closest available altitude data point using the following barometric conversion equation [41]:

$$\rho_{hub} = \left(\frac{p_{closest}}{100} - (h_{hub} - h_{closest})\cdot\frac{1}{8}\right)\cdot\frac{\rho_{ambient}\cdot T_{ambient}\cdot 100}{p_{ambient}\cdot T_{hub}} \tag{9}$$

where ρ is air density (kg/m^3) and p is air pressure (Pa). WindPowerLib then corrects the wind speeds for wake losses by applying the *Knorr* mean wind efficiency curve, which is constructed by averaging empirically found wind efficiency curves of over 2000 wind parks in Germany [42]. Next, the library converts the adjusted wind speed profile to an electricity supply profile using the power curve appointed to the turbine in Section 2.2. Here, the power curve states the electricity output for incremental hub height wind speeds (in steps of 0.5 m/s). The power curve is air density corrected each time step using the following equation [43–45]:

$$U_{corrected} = U_{original} * \left(\frac{\rho_{ambient}}{\rho_{hub}}\right)^{a} \tag{10}$$

with:

$$a = \begin{cases} \frac{1}{3} & U_{original} \le 7.5\ \text{m/s} \\ \frac{1}{15} * U_{original} - \frac{1}{6} & 7.5\ \text{m/s} < \text{U}_{\text{original}} < 12.5\ \text{m/s} \\ \frac{2}{3} & U_{original} \ge 12.5\ \text{m/s} \end{cases} \tag{11}$$

where $U_{original}$ is a certain wind speed value in the original power curve and $U_{corrected}$ is the corresponding wind speed value in the air density corrected power curve. The correction accounts for the fact that a higher wind speed is required for a certain power output when air density is lower than ambient (1.225 kg/m^3), and vice versa. The resulting electricity supply profile is multiplied by the earlier assigned turbine power scaling factor to account for the discrepancy in rated power mentioned in Section 2.2.1. Additional (constant) correction factors are applied to account for losses due to downtime, operational electrical efficiency, turbine electricity consumption, blade contamination and degradation, adverse weather and cut-out recovery time [46] (see Table 3, last column). Finally, the turbine capacity factor (CF) is calculated using the following equation:

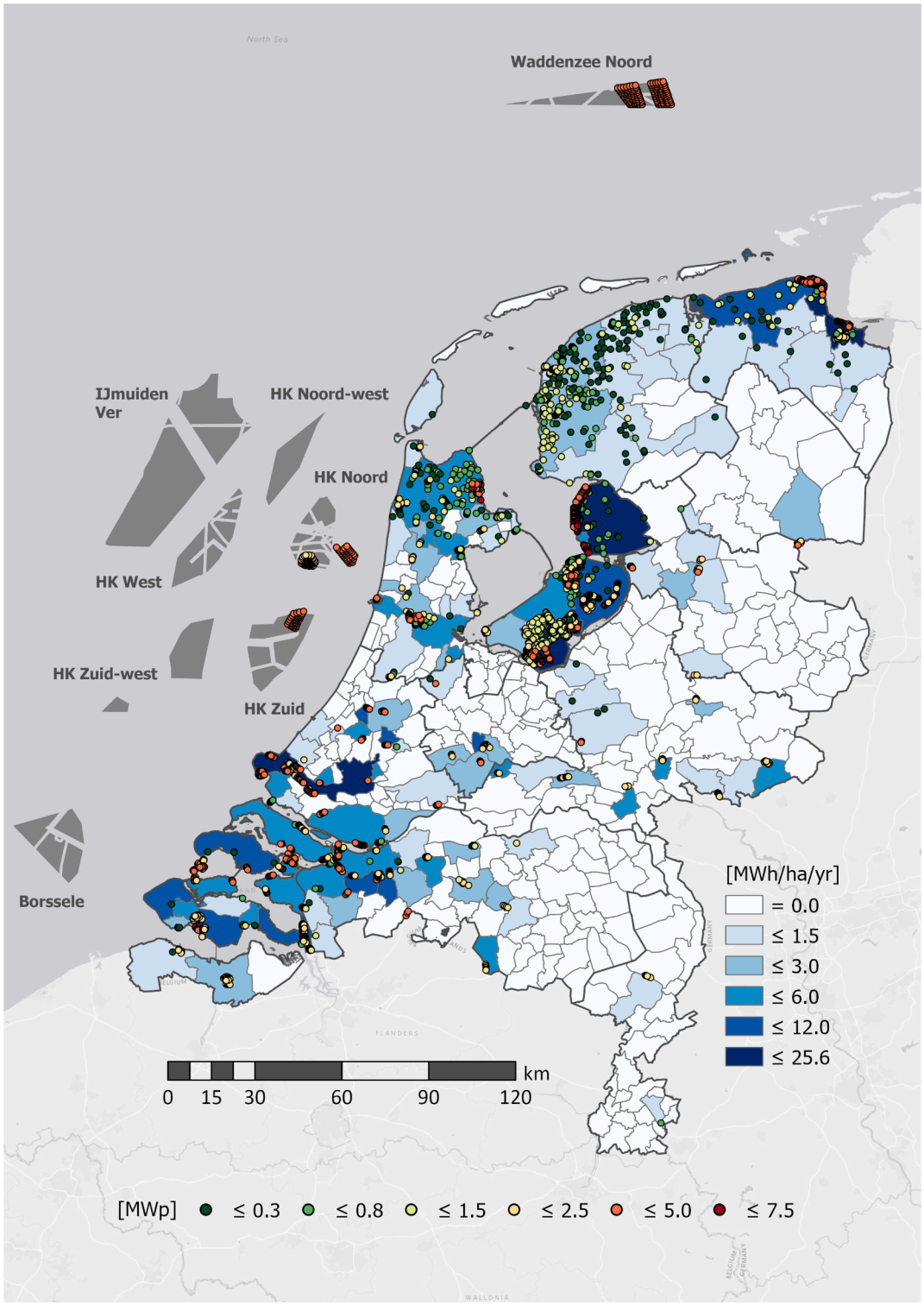

Fig. 2. Geographical distribution of wind turbines and their municipality level electricity generation densities, for the present-day situation (2019). Basemap service layer credits: Esri, DeLorme, HERE, MapmyIndia. Offshore wind exploration areas layer credits: RWS.

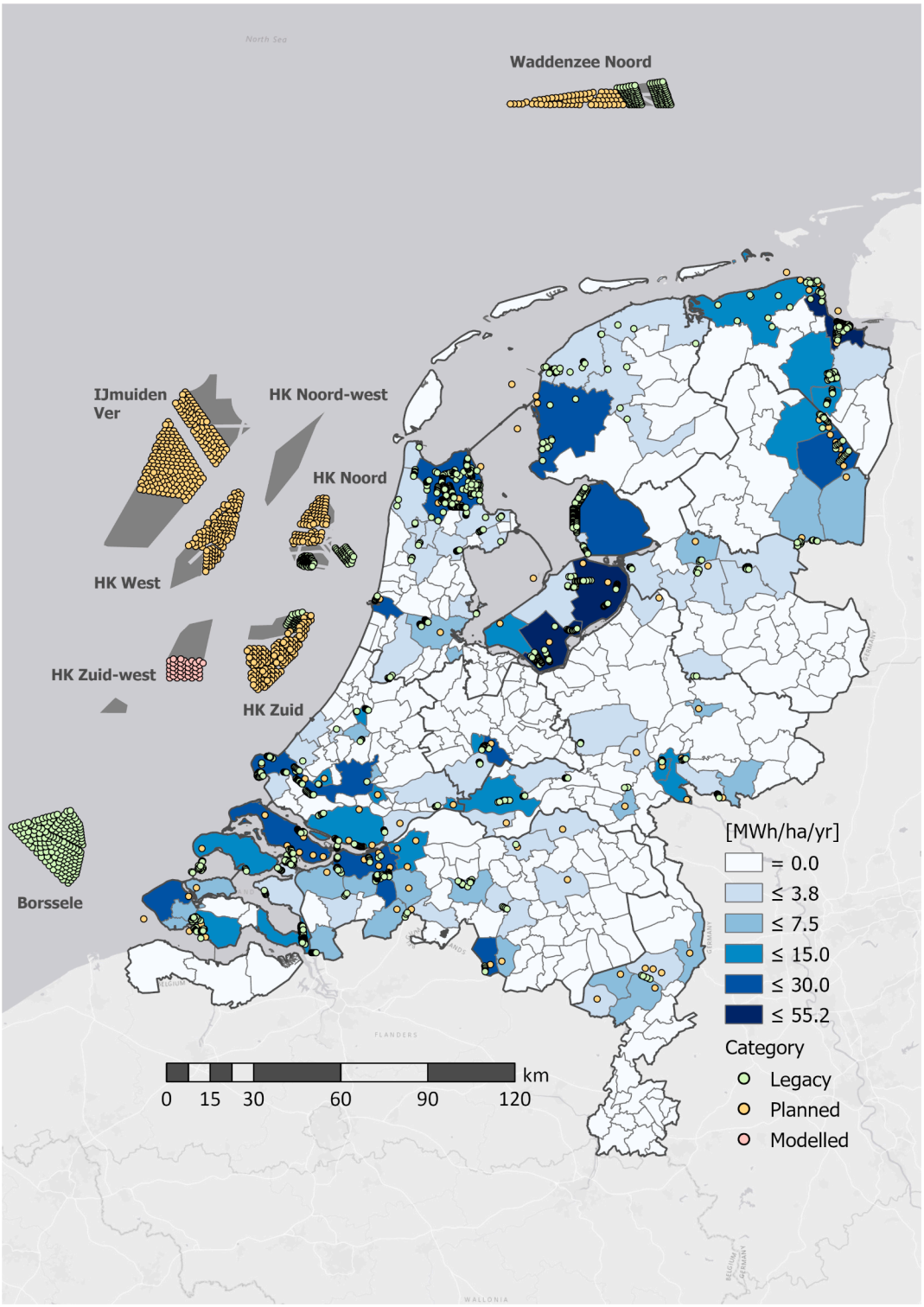

Fig. 3. Geographical distribution of wind turbines and their municipality level electricity generation densities, for the 2030 Climate Agreement scenario. Basemap service layer credits: Esri, DeLorme, HERE, MapmyIndia. Offshore wind exploration areas layer credits: RWS.

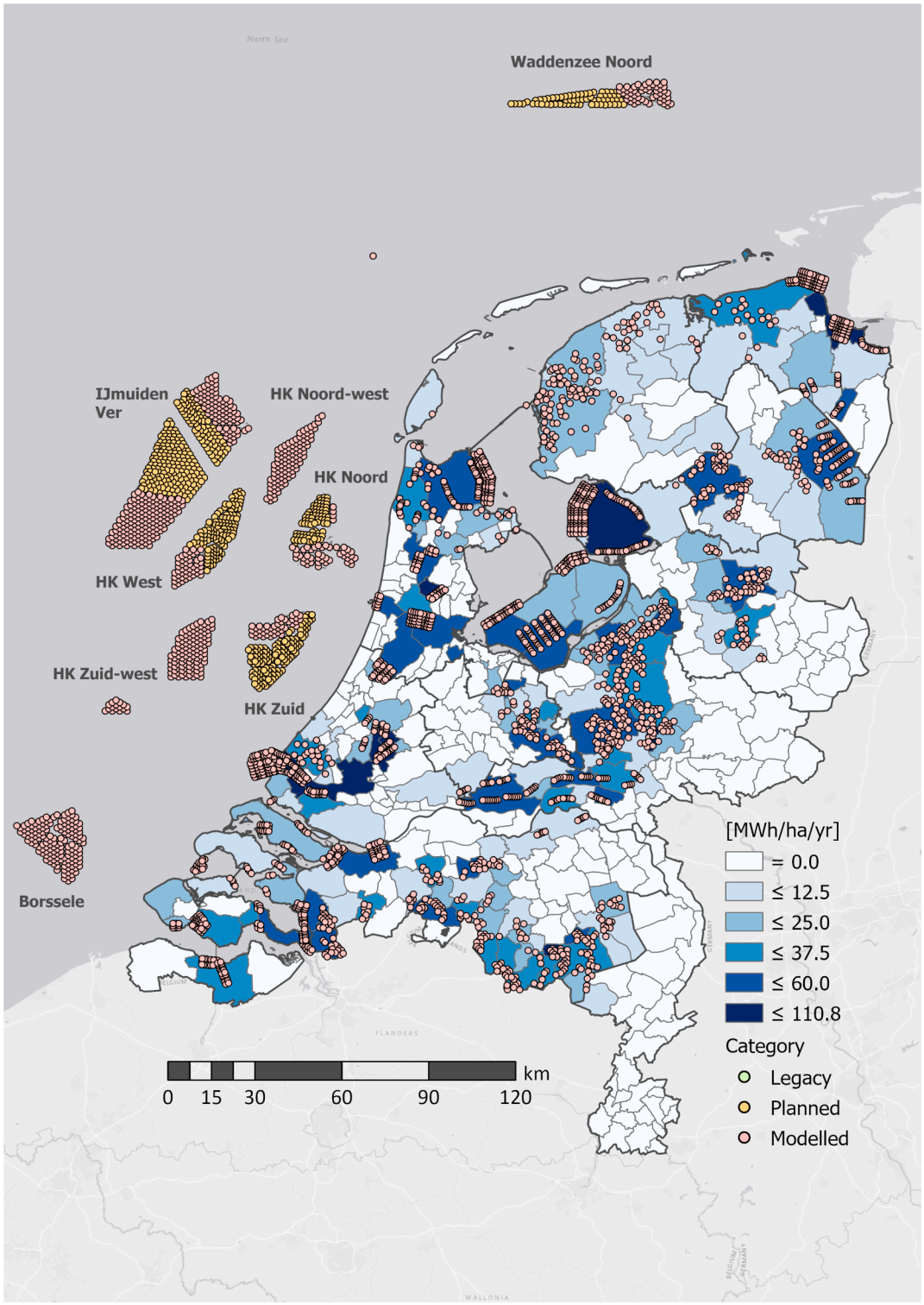

Fig. 4. Geographical distribution of wind turbines and their municipality level electricity generation densities, for the 2050 Regional Steering scenario. Basemap service layer credits: Esri, DeLorme, HERE, MapmyIndia. Offshore wind exploration areas layer credits: RWS.

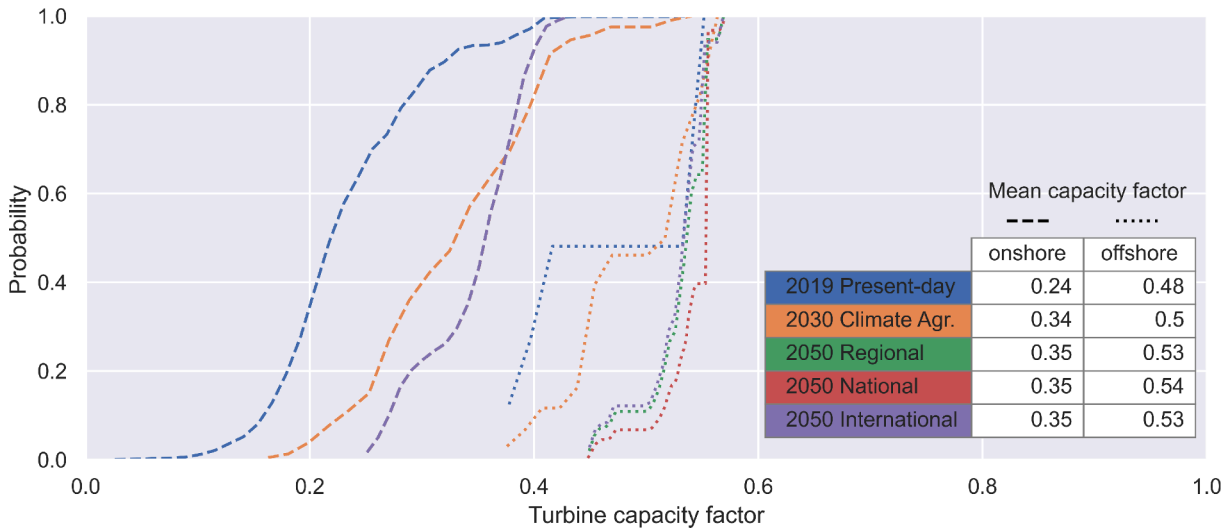

Fig. 5. Cumulative distribution functions (CDF) of onshore (dashed lines) and offshore (dotted lines) wind turbine capacity factors for all scenarios. Note that the onshore Regional Steering line is identical to the National Steering one. Mean capacity factors are shown in the embedded table.

$$CF_{turbine} = \frac{E_{calculated,\,turbine,\,annual}}{E_{rated,\,turbine,\,annual}} \tag{12}$$

with:

$$E_{rated,\,turbine,\,annual} = P_{rated,\,turbine} \cdot 60\,[\mathrm{s}] \cdot 60\,[\mathrm{min}] \cdot 24\,[\mathrm{h}] \cdot 365\,[\mathrm{days}] \tag{13}$$

where $E_{calculated}$ is the electricity output as calculated in the WEM and E_{rated} the electricity output if the turbine was to be continuously operating at rated power.

3. Results

3.1. Turbine maps

For the present-day situation (2019), Fig. 2 shows 2015 onshore turbines with a combined rated power of 3.48 GWp (1.73 MWp average) and 289 offshore turbines with a combined rated power of 0.96 GWp (3.31 MWp average). This amounts to a total of 2304 turbines with a combined capacity of 4.43 GWp (1.92 MWp average). Exactly matching power curves are found for 1665 of these turbines (72.3%). The remaining 639 turbines (27.7%) are assigned power curves belonging to the most similar commercially available turbine model (see Section 2.2.1). The geographical distribution of the onshore turbines is far from uniform. One can roughly divide the country through a Southwest-Northeast diagonal creating a northwestern part which is turbine rich and a southeastern part which is largely devoid of turbines. This roughly correlates with the wind resource differences over the country. The province of Friesland shows a very large and mostly unstructured cluster of lower capacity turbines (see Fig. A.1 for an overview of Dutch provinces). The provinces of Groningen and Noord-Holland show similar clusters (although considerably less dense in Groningen) accompanied by a couple of small clusters of high capacity turbines. Compact clusters of both lower and very high capacity turbines translate to remarkably high capacity densities in the province of Flevoland. Especially note the structured land-water-nexus alignments of large turbines in the northern part of the province. With the notable exception of the Amsterdam and Rotterdam harbors, the Randstad area (the mid-western part of the country) is only dotted with small alignments of mostly medium to large capacity turbines. The southwestern delta region again shows high capacity densities, which can mostly be attributed to multiple newer alignments of large turbines. Regarding offshore turbines, only three wind exploration areas (darker gray polygons) are partially utilized in the present-day situation: Hollandse Kust Zuid, Hollandse Kust Noord and Waddenzee Noord.

Considering the 2030 situation, Fig. 3 depicts 1938 onshore turbines with a combined rated power of 6.20 GWp (3.20 MWp average) and 1197 offshore turbines with a combined rated power of 11.41 GWp (9.53 MWp average). This totals up to 3135 turbines with a combined capacity of 17.60 GWp (5.61 MWp average). Still operational present-day turbines (green dots) make up 47.3% (2.9 GWp) of the onshore capacity. The remaining 52.7% (3.3 GWp) is accounted for by planned SDE+ turbines (orange dots). The considerable increase in onshore average turbine capacity compared to the present-day situation can be attributed to two factors: the present-day turbines that are still operational in 2030 are generally larger (3.06 MWp average) than the ones that are decommissioned by 2030 (1.29 MWp average); and the capacities of the newly commissioned SDE+ turbines are relatively high (3.33 MWp average). Since all turbines that are part of a certain SDE+ park are placed at the exact same location (see Section 2.2.2), the (stacked) orange onshore dots represent wind parks rather than individual turbines. Keep in mind that this creates the appearance of a less saturated landscape. The province of Friesland sees a shift in capacity concentration towards the west. This can be explained by the decommissioning of most of it's present-day turbines in combination with the commissioning of many larger SDE+ turbines around it's west coast. Repowering and expansion of wind parks in and around Eemshaven and Delfzijl further increase the high capacity density in the northeastern part of the province of Groningen. A section of the border between the provinces of Groningen and Drenthe that was first devoid of turbines now shows high capacity densities. With the notable exception of the Ijmuiden harbor, the province of North-Holland sees general shift in capacity towards the northeastern-most part. The mainland part of the province of Flevoland sees a decommissioning of all inland turbines and no new turbines replacing them. Only the land-water-nexus alignments of large turbines remain operational. Despite the decommissioning of many present-day turbines, the island part of the province of Flevoland sees regions with drastically increased capacity densities due to the realization of a couple of very large SDE+ wind parks. The northern part of the province of Zuid-Holland sees a partial decommissioning of present-day turbines and no commissioning of new turbines, resulting in an even less saturated landscape. The Rotterdam harbor remains a scene of considerable amounts of large turbines. Due to their relatively low age, many present-day turbines remain operational in the southwestern delta region. Complemented by considerable amounts of new SDE+ turbines, the region shows a further increase in capacity densities. Even though the Dutch interior remains generally turbine poor, multiple

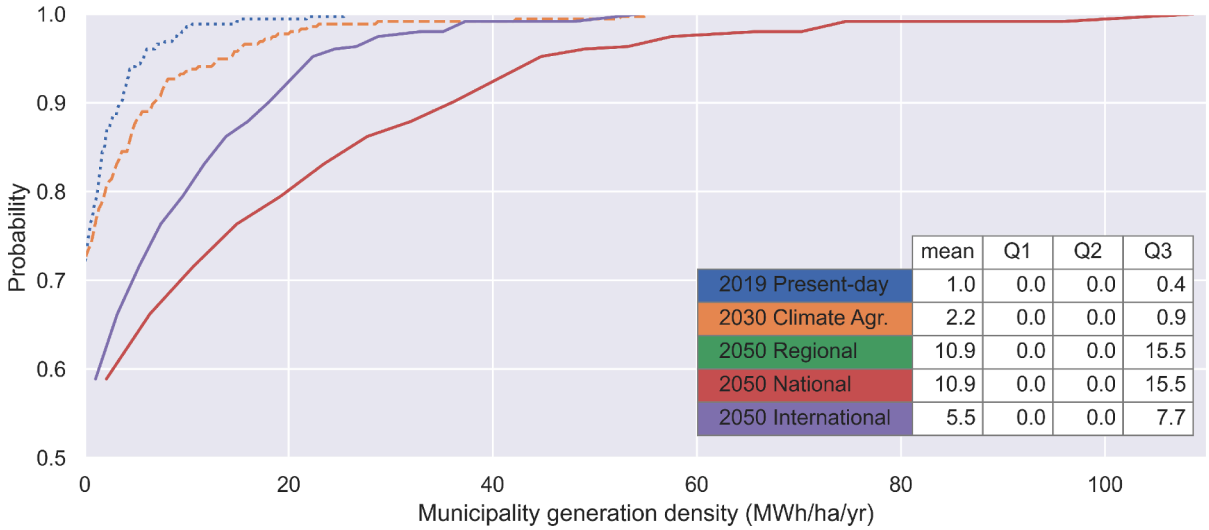

Fig. 6. Cumulative distribution functions (CDF) of municipality wind electricity generation densities for all scenarios. The dotted line represents the present-day situation, the dashed line the 2030 situation and the solid lines the three 2050 situations. Note that the Regional Steering line is identical to the National Steering one. Mean and quartile generation density values are shown in the embedded table.

Table 4
Total wind electricity generation (TWh/yr) per shore type for each energy transition scenario.

Scenario	Generation onshore	Generation offshore	Generation country
2019 Present-day	8.3	4.2	12.5
2030 Climate Agreement	18.8	50.9	69.6
2050 Regional Steering	61.4	145.3	206.8
2050 National Steering	61.4	244.8	306.3
2050 International Steering	30.7	128.3	159.1

notable areas of turbine development can be distinguished in the provinces of Overijssel, Gelderland and Limburg. Regarding offshore wind capacity, 21.6% (2.5 GWp) is accounted for by still operational present-day parks (green dots), 72.6% (8.3 GWp) by planned parks with officially suggested layouts (orange dots) and 5.8% (0.7 GWp) by parks without officially suggested layouts that are therefore algorithm generated (red dots). Of the wind exploration areas, Borssele and Waddenzee Noord are already fully utilized by 2030. Though considerably developed, Ijmuiden Ver and Hollandse Kust Noord, Zuid, West and Zuid-west offer varying degrees of room for expansion later on. Hollandse Kust Noord-west has yet to see its first turbine development.

For the 2050 Regional Steering scenario, Fig. 4 shows 2254 onshore turbines with a combined rated power of 20.0 GWp (8.87 MWp each) and 2205 offshore turbines with a combined rated power of 31.0 GWp (14.1 MWp average). This amounts to a total of 4459 turbines with a combined capacity of 51.0 GWp (11.4 MWp average). Keep in mind that the locations of all onshore turbines are adopted from the book *Energie en Ruimte* [38] which depicts a possible future distribution that does not consist of actually planned wind parks. Though still showing a clustered nature, the onshore turbines are more evenly spread over different parts

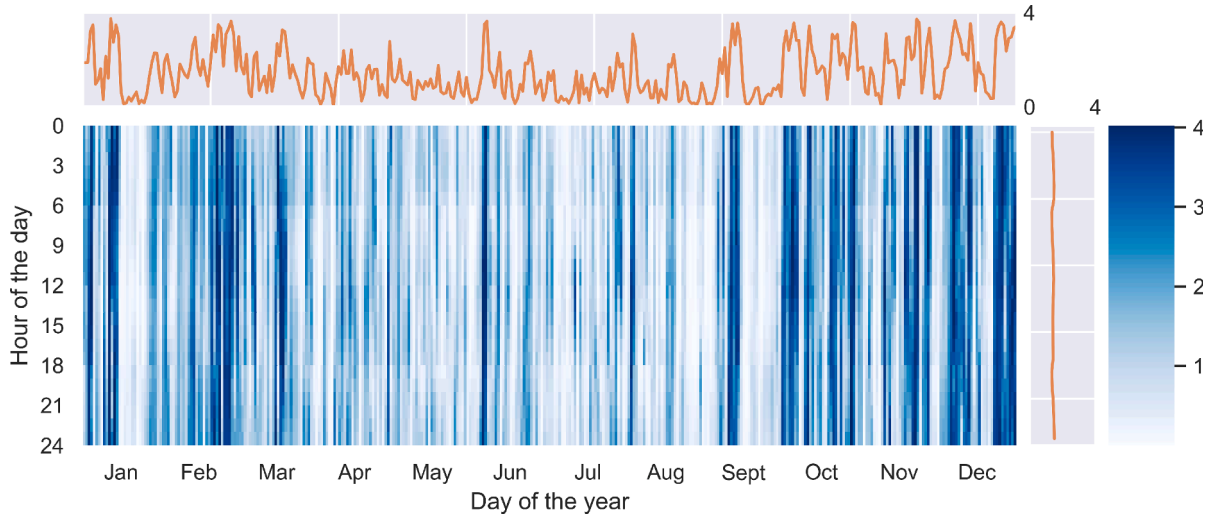

Fig. 7. Heatmap of country-level wind turbine power output [GW] for the present-day situation (2019).

Table 5
Seasonal present-day (2019) wind electricity generation considering different meteorological years as input. Absolute [GWh] as well as relative to long-term averages (LTA) values.

	Winter		Spring		Summer		Autumn		TOTAL	
Meteo input	abs	rel	abs	rel	abs	rel	abs	rel	abs	rel
2008	4,346	(1.031)	3,307	(1.161)	2,604	(1.172)	3,524	(1.084)	13,781	(1.099)
2009	3,532	(0.838)	2,816	(0.988)	2,235	(1.006)	3,795	(1.167)	12,377	(0.987)
2010	3,127	(0.742)	2,653	(0.931)	1,851	(0.833)	3,239	(0.996)	10,870	(0.867)
2011	4,606	(1.093)	2,691	(0.944)	2,496	(1.124)	3,354	(1.032)	13,147	(1.049)
2012	4,419	(1.048)	2,512	(0.882)	2,361	(1.063)	3,201	(0.985)	12,492	(0.997)
2013	3,958	(0.939)	3,079	(1.080)	2,033	(0.915)	3,288	(1.011)	12,357	(0.986)
2014	5,116	(1.214)	2,721	(0.955)	2,019	(0.909)	2,614	(0.804)	12,470	(0.995)
2015	4,747	(1.126)	3,131	(1.099)	2,426	(1.092)	3,389	(1.043)	13,693	(1.092)
2016	4,244	(1.007)	2,896	(1.016)	2,041	(0.919)	2,529	(0.778)	11,710	(0.934)
2017	4,049	(0.961)	2,689	(0.944)	2,144	(0.965)	3,573	(1.099)	12,456	(0.994)
LTA	4,214		2,849		2,221		3,251		12,536	

Table 6
Relative error [%] of country-level wind electricity generation per shore type and season (2017).

Shore type	Winter	Spring	Summer	Autumn	Year
Onshore	+14.4	+ 1.8	− 1.6	+ 14.1	+ 8.7
Offshore	+10.0	+ 22.9	+ 18.9	+ 4.3	+ 12.7
Combined	+12.9	+ 9.2	+ 5.6	+ 10.5	+ 10.1

of the country when compared to the present-day or 2030 situation. The considerably higher saturation of the Dutch interior is largely due the development of so-called wind forests - relatively widely spaced swarms of turbines towering above production forests - in the provinces of Drenthe, Overijssel, Gelderland, Utrecht and Noord-Brabant. Additionally, a multitude of relatively short river alignments amount to considerable capacity densities in the southwestern part of the province of Gelderland. Also the center and northern parts of the province of Zuid-Holland, which were rather turbine poor in the present-day and 2030 situation, see the development of multiple new wind parks. The traditionally turbine rich parts of the country are subject to repowering: the process of replacing many relatively small turbines with a lower number of relatively large turbines that amount to a higher total capacity [38]. Especially note the extremely high capacity densities of the Eemshaven, the Rotterdam harbor and the mainland part of the province of Flevoland. Planned offshore wind parks with officially suggested layouts (orange dots) are assumed to remain operational and account for 26.7% (8.3 GWp) of total offshore wind capacity in 2050. The algorithm generated turbines that repower all present-day parks and fill-up the remaining space of the wind exploration areas (red dots) account for another 40.8% (12.63 GWp). The remaining 32.5% (10.1 GWp) could not be fitted into the wind exploration areas and are therefore allocated to the arbitrary location north-west of Vlieland (see Section 2.2.5). Maps for the other two 2050 scenarios (National and International Steering) can be found in Appendix B.

3.2. Turbine electricity generation

In addition to turbine locations and characteristics, Figs. 2–4 show calculated onshore wind electricity generation densities (MWh/ha/yr) on a municipality level. These generation densities obviously correlate with the capacity densities as described in the previous section. Deviations from this relationship can be explained through differences in turbine capacity factor: the annually averaged power output divided by the rated power. Fig. 5 displays these capacity factors in the form of cumulative distribution functions (CDFs) which indicate the probability that a randomly selected turbine has a capacity factor equal to or lower than the value on the x-axis. It does this for each scenario and both shore classes (onshore and offshore). Note that the onshore Regional Steering line is not visible, since it is identical to the National Steering one. Two determining factors become apparent; offshore turbines generally have a higher capacity factor compared to onshore turbines and future turbines generally have a higher capacity factor compared to present-day turbines. These factors can be used to explain the differences in country level capacity factor between the scenarios, which are 0.32, 0.45, 0.46, 0.49 and 0.48 for respectively the present-day, 2030 Climate Agreement, 2050 Regional, 2050 National and 2050 International situations. Turbines within the same scenario and shore class also show considerable internal variation in capacity factor, which reflects the geographically varying ratio between regional capacity density and generation density.

The municipality-level generation densities shown in Figs. 2–4 are also displayed in the form of CDFs in Fig. 6. The table embedded in the figure provides a numeric version of the graph, stating mean, first quartile, second quartile (also called median) and third quartile density values. Note that the Regional Steering line is not visible, since it is identical to the National Steering one. For all scenarios, the figure shows a majority of municipalities without any electricity generation (first two quartiles are zero), reflecting the earlier mentioned tendency to geographically cluster wind turbines. For the municipalities that do have generation, all scenarios show a logarithmic shape, indicating decreasing representation of municipalities with increasingly large generation densities. The logarithmic shapes are more flattened for the 2050 scenarios, indicating more equal distributions. Through time, a clear growth in mean generation density can be perceived, most notably when following the Regional Steering and National Steering pathways.

Table 4 presents the total onshore, offshore and country-level wind electricity generation for the present-day situation and all energy transition scenarios. Compared to the present-day situation, the country-level generation is a factor 16.6, 24.6 or 12.8 higher in 2050 when respectively applying Regional, National or International Steering. In addition, two alternative present-day runs have been performed; one where wind speeds are not corrected for wake losses and one where the power curves are not air density corrected (see Section 2.3). These runs indicate that present-day country-level generation is reduced with 5.1% by performing wake loss correction (6.0% for onshore and 3.3% for offshore) and increased with 0.6% by performing air density correction (0.6% for onshore and 0.4% for offshore).

Providing insight in the temporal component of wind electricity generation, Fig. 7 features a heatmap (blue) displaying the present-day country-level power output for each hour of the day (*y*-axis) for each day of the year (*x*-axis). The accompanying line graphs (orange) show the averaged power output per day of the year (horizontal graph) and per hour of the day (vertical graph). On average, autumn and winter show much higher power output compared to spring and especially summer. Nevertheless, the horizontal line graph shows that the day-to-day variation is high throughout the year and days with close to zero power as well as days with close to rated power can be found in each season. It is the frequencies with which these type of days occur that distinguish the

seasons. When averaged over the year, the different parts of the day show only minor differences in output power between them. However, for separate days, the differences between the morning, afternoon, evening and night can be considerable.

In order to gain an understanding of the inter-annual variability in wind electricity generation, the model is run for a series of 10 meteorological years (2008–2017) assuming the same present-day capacity distribution (2019). Table 5 presents the resulting country-level generation per season for each meteorological year. Compared to the long-term average (LTA), yearly generation is shown to deviate within a range of − 13.3% (2010) to +9.9% (2008) and seasonal generation within a range of − 25.8% (winter 2010) to +21.4% (winter 2014). The meteorological year that is assumed for all scenarios during this research (2017) shows the second smallest yearly deviation (− 0.6%) and the smallest average absolute seasonal deviation (5.7%), and can therefore be considered typical.

Finally, the model is run for the year 2017, regarding both capacity distribution and meteorology. This time, the turbine fleet is made dynamic over time; electricity generation is modeled for a turbine during the part of the year that it was operational [29]. For example, if a turbine was constructed on November 1st 2017, electricity generation is only modeled for the last two months of the year. The modeled country-level electricity generation is validated against a dataset on registered historical electricity generation [47]. Table 6 presents the resulting relative errors [%] per shore type and season. While winter and autumn show considerably higher errors than spring and summer for the onshore turbines, the opposite is true for the offshore turbines. Considering the year as a whole, the onshore turbines display a lower error (+8.7%) than the offshore turbines (+12.7%). Overall, the modeled generation is higher than the registered generation (+10.1%). A lower modeled generation is only shown for the onshore turbines during summer (− 1.6%).

4. Discussion

The developed wind energy module has some limitations and uncertainties, which are discussed in this section. Regarding the construction of the 2030 onshore turbine map, all currently planned SDE+ wind parks are assumed to be realized. It is likely however, that some of these projects will be withdrawn during preparatory phases due to legal issues or growing societal opposition to onshore wind park realization. Furthermore, the SDE+ dataset does not specify whether or not a wind project concerns repowering. It can therefore occur that certain present-day turbines, which will in reality make way for SDE+ parks, are not decommissioned in the model since they have not yet reached the assumed average lifetime of 20 years by 2030. This would result in erroneous double occupancy of land. Moreover, while the effect on modeled electricity generation is expected to be limited, the placement of SDE+ parks at the centroids of town polygons is often not realistic in geographical sense. While the above mentioned elements impose uncertainties regarding the placement of onshore turbines in 2030, the current methodology does allow for automatic and rapid updating of the map whenever a new version of the SDE+ dataset becomes available. This would not be the case if additional details (such as the exact location and whether or not it concerns repowering) were to be manually sorted out for each planned SDE+ park.

The geographical distribution of onshore turbines in 2050 is highly uncertain, since it cannot be deduced from locations of present-day turbines or already planned but not yet realized wind parks. The distribution selected for this research should therefore be seen as a possible rather than probable one. Moreover, assuming the same distribution and therefore the same number of turbines for scenarios with highly different total onshore capacities is somewhat problematic, as it can result in rather high average onshore turbine capacities (8.87 MWp for both Regional and National Steering). In turn, this might lead to unrealistic rotor diameter versus hub height ratios, as the hub height for all turbines in 2050 are assumed to be identical (100 m).

Given the chosen layouts and turbine spacings, the wind exploration areas considered in the current model can harbor 20.9 GWp of offshore capacity in 2050. The remaining offshore capacity (10.1 GWp, 30.6 GWp and 6.6 GWp for respectively the Regional, National and International Steering scenario) is assigned to an arbitrary location. Additional wind exploration areas have been suggested by the Netherlands Enterprise Agency (RVO). In a recent study, Blix Consultancy estimated that these areas could fit another 54.0 GWp of offshore wind [48], more than enough to accommodate the remaining offshore capacity in all 2050 scenarios. This suggests that incorporation of the additional exploration areas in a next version of the model would obviate the need to assign offshore turbines to arbitrary locations.

Considering the calculation of electricity generation, the same mean wind efficiency curve is applied to all turbines during all hours of the year. In reality, these curves are dependent on relative turbine positioning as well as wind direction and do therefore vary between turbines and hours of the year. Explicit modeling of wake related wind speed reductions would allow for more realistic electricity generation profiles. However, this does require an exact layout for each wind park, which is currently lacking for the SDE+ projects.

Factors that are worth looking into when trying to find explanations for the described discrepancies between modeled and registered wind electricity generation include; errors in the 3D meteorological dataset, assignment of not exactly matching power curves, over-optimistic power curves (provided by manufacturers) and application of non-representative loss factors. On the other hand, the registered wind electricity dataset itself partly consists of estimated data (were measurement could not be obtained) [47] and might therefore deviate from reality on its own. In addition, it is relevant to know how far up the electricity grid the measurements were performed, since this influences the magnitude of grid losses (which are outside the scope of the WEM).

As mentioned in the introduction, the ASM2 model (and therefore the WEM) currently focuses on analyzing energy system performance in terms of electricity flows. Integrating detailed economic, environmental and GHG emission analyses would result in a more complete picture of the profitability of the energy transition scenarios. Furthermore, the WEM is currently a completely deterministic model. Incorporation of artificial intelligence could further enhance the selection of turbine types, heights and locations by optimizing for net present value. In the overlapping ASM2 model, optimization algorithms that determine cost-optimal deployment and management of regional energy storage systems are already successfully incorporated.

In principle, the methodology proposed in this research can also be applied to other areas around the word. The WEM does rely on a multitude of area-specific input datasets though, ranging from 3D meteorological time series to overviews of planned but not yet realized wind parks. In case one or more of these datasets is not available for the area of interest, custom workarounds must be developed and incorporated.

5. Conclusions

In conclusion, a wind energy module is developed which is capable of constructing geodatabases of hourly onshore and offshore wind electricity generation profiles on a turbine level for the present-day, the near future (2030) and the distant future (2050), based on available top-down scenarios. The capability of constructing not only temporally but also spatially resolved future generation profiles underscores the added value of the WEM, as it allows for more in-depth analysis of grid congestion, energy storage and hydrogen production in future Dutch energy systems. For the geographical distribution of turbine capacity, the module utilizes datasets on historically operational turbines, planned wind parks and possible future turbine distributions. Turbine electricity generation profiles are constructed using a high resolution 3D meteorological dataset and power curves of commercially available turbine models. They are corrected for air pressure deviations and a multitude of loss factors, including wake effects. The wind energy module can be easily updated when new versions of input datasets become available and re-runs for alternative energy transition scenarios (supporting updated policy options) or meteorological years are straightforward. The following answers to the research questions are found:

Q1. What are the projected regional developments in onshore and offshore wind turbine capacity? While the number of onshore turbines is projected to decrease slightly towards 2030 (from 2015 to 1938), their combined rated power increases considerably (from 3.48 GWp to 6.20 GWp) due to an increase in average rated power (from 1.73 MWp to 3.20 MWp). Geographical shifts in onshore turbine capacity concentration are projected for the provinces of Friesland (towards the west), Groningen (towards the northeast), Noord-Holland (towards the northeast) and Flevoland (towards the south). Although the Dutch interior remains largely turbine poor, notable areas of turbine development are projected for the provinces of Overijssel, Gelderland, Limburg and especially Drenthe. Despite these shifts and developments, the southwestern delta region, the Ijsselmeer region and the coastal part of the province of Groningen remain the major onshore capacity hot-spots in 2030. Regarding the offshore situation, large increases are projected towards 2030 for the number of turbines (from 289 to 1197), their average rated power (from 3.31 MWp to 9.53MWp) and their combined rated power (from 3.31 MWp to 9.53 MWp). While most offshore wind exploration areas offer varying degrees of room for expansion later on, Borselle and Waddenzee Noord are projected to already be fully utilized by 2030.

While the number of onshore turbines in 2050 are projected to be the same for the Regional, National and International Steering scenarios (2254), their combined rated power varies greatly (20.0, 20.0 GWp and 10.0 GWp, respectively) due to differences in average rated power (8.87 MWp, 8.87 MWp and 4.44 MWp, respectively). Compared to the present-day and 2030 situations, the onshore turbines are projected to be more evenly spread over different parts of the country. This can be attributed to the development of multiple wind forests, river alignments and other types of wind parks in the Dutch interior and the province of Zuid-Holland. The traditionally turbine rich parts of the country are subject to repowering, greatly increasing their wind capacity densities. Various degrees offshore wind development are projected for the Regional, National and International Steering scenarios regarding the number of turbines (2205, 3572 and 1972 respectively), their average rated power (14.1 MWp, 14.4 MWp and 13.9 MWp respectively) and their combined rated power (31.0 GWp, 51.5 GWp and 27.5 GWp respectively). In all scenarios, every offshore wind exploration area considered in this research is projected to be fully utilized by 2050.

Q2. What is the temporally resolved electricity generation of this wind turbine capacity under typical meteorological circumstances? Assuming identical meteorological circumstances (2017), country-level wind electricity generation is projected to increase from 12.5 TWh/yr in 2019 to 69.6 TWh/yr in 2030 to either 206.8 TWh/yr, 306.3 TWh/yr or 159.1 TWh/yr in 2050 when respectively following the Regional, National or International Steering pathway. Logically, regional electricity generation densities follow the above discussed capacity densities in all scenarios. Deviations from this relationship can be explained through differences in turbine capacity factor, which is shown to be generally higher for offshore (versus onshore) and future (versus present-day) turbines. While autumn and winter generally show much higher power output compared to spring and especially summer, the day-to-day variation is high throughout the year and days with close to zero power as well as days with close to rated power can be found in each season for all scenarios. And while different parts of the day show only minor difference in output when averaged over the year, the variation between morning, afternoon, evening and night can be considerable for separate days. Compared to the long-term average, yearly wind electricity generation is shown to deviate within range of − 13.3% to +9.9% and seasonal generation within a range of − 25.8% to +21.4% when assuming the same present-day (2019) capacity distribution for different meteorological years (2008–2017).

The most prominent recommendations for future research follow from the discussion. This includes the addition of the newly suggested offshore wind exploration areas and the integration of economic, environmental and GHG emission analyses. Incorporating artificial intelligence in the form of optimization algorithms is also recommended when aiming to further improve the module. Finally, might an alternative model be developed (by another research team) that is also capable of constructing Dutch spatiotemporal wind generation profiles, it is recommended to perform a thorough comparison between the two models in terms of methodology and results.

Funding

This work was supported by the Ministry of Economic Affairs and Climate Policy via the Topsector Energy project Advanced Scenario Management 2 (project TEUE116903).

CRediT authorship contribution statement

N.S. Nortier: Conceptualization, Methodology, Investigation, Writing – original draft, Visualization. **K. Löwenthal:** Methodology, Investigation. **S.L. Luxembourg:** Methodology, Investigation, Writing – review & editing. **A. van der Neut:** Methodology, Investigation. **A.A. Mewe:** Conceptualization, Writing – review & editing. **W.G.J.H.M. van Sark:** Conceptualization, Methodology, Investigation, Writing – review & editing.

Declaration of Competing Interest

Authors declare that they have no conflict of interest.

Acknowledgments

The authors would like to thank Bosch & van Rijn and Vereniging Deltametropool for sharing data valuable to this research.

Appendix A. Dutch provinces and wind exploration areas

Fig. A.1. Dutch provinces (colored, layer credits: Esri Nederland, CBS) and offshore wind exploration areas (dark gray, layer credits: RWS). Basemap service layer credits: Esri, DeLorme, HERE, MapmyIndia.

Appendix B. Additional turbine location and electricity generation maps

This appendix displays the turbine location and electricity generation maps for the 2050 National and International Steering scenarios. For the 2050 National Steering scenario, Fig. B.1 shows 2254 onshore turbines with a combined rated power of 20.0 GWp (8.87 MWp each) and 3572 offshore turbines with a combined rated power of 51.5 GWp (14.4 MWp average). This amounts to a total of 5826 turbines with a combined capacity of 71.5 GWp (12.3 MWp average). For the 2050 International Steering scenario, Fig. B.2 shows 2254 onshore turbines with a combined rated power of 10.0 GWp (4.43 MWp each) and 1972 offshore turbines with a combined rated power of 27.5 GWp (13.9 MWp average). This totals up to 4226 turbines with a combined capacity of 37.5 GWp (8.87 MWp average).

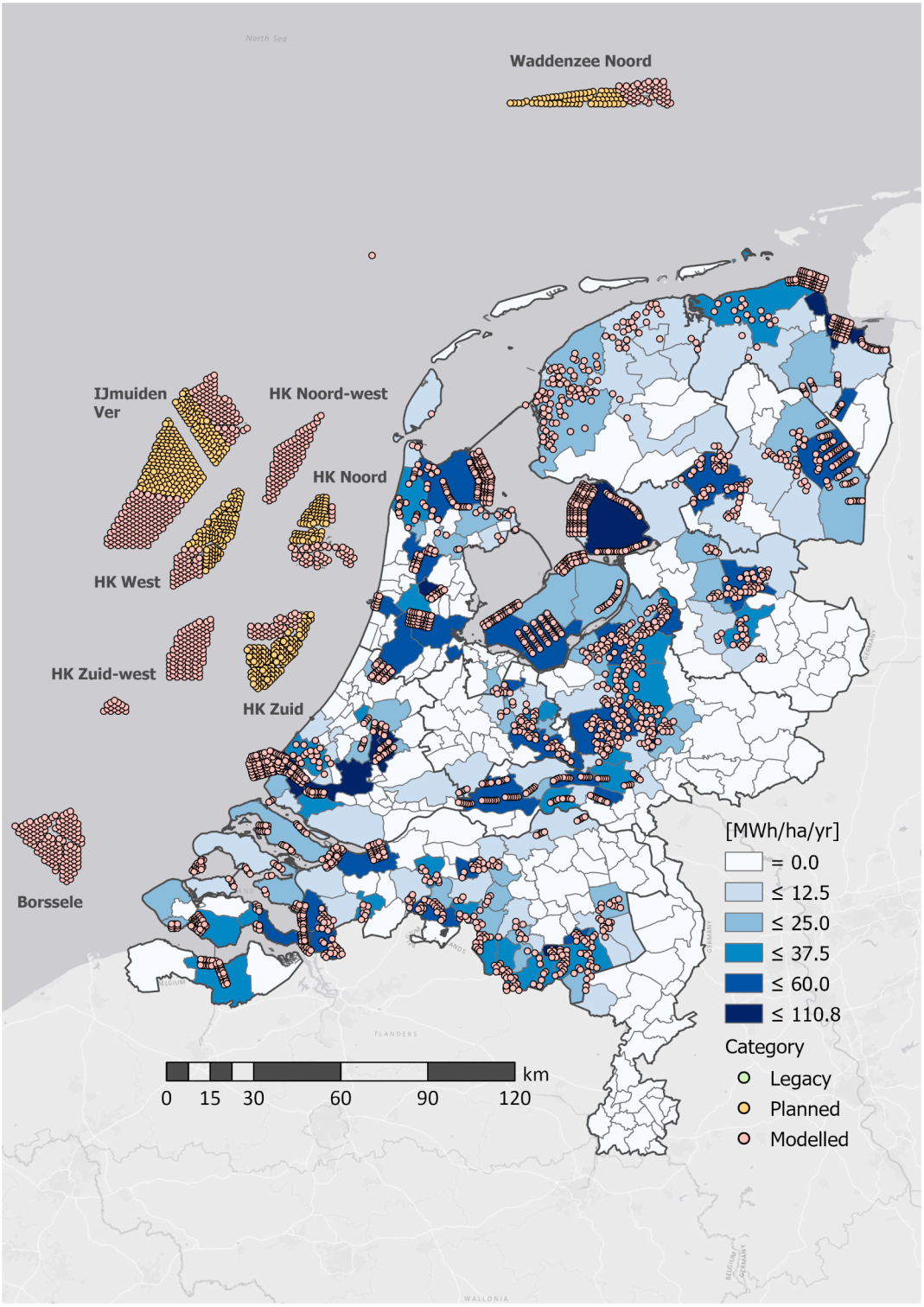

Fig. B.1. Geographical distribution of wind turbines and their municipality level electricity generation densities, for the 2050 National Steering scenario. Basemap service layer credits: Esri, DeLorme, HERE, MapmyIndia. Offshore wind exploration areas layer credits: RWS.

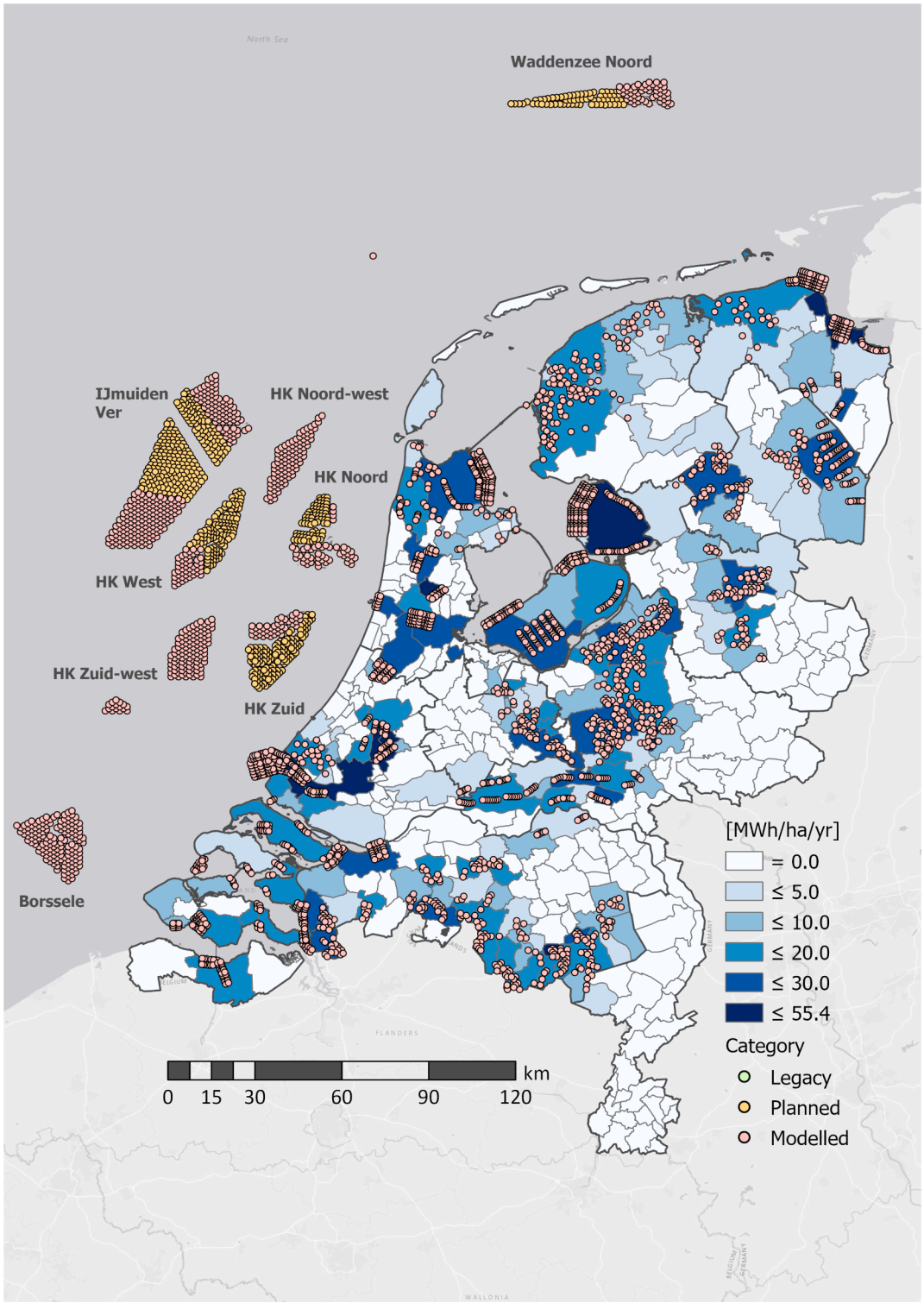

Fig. B.2. Geographical distribution of wind turbines and their municipality level electricity generation densities, for the 2050 International Steering scenario. Basemap service layer credits: Esri, DeLorme, HERE, MapmyIndia. Offshore wind exploration areas layer credits: RWS.

References

[1] Center for Climate and Energy Solutions, Outcomes of the U.N. Climate Change Conference in Paris. Technical Report, Center for Climate and Energy Solutions, 2015.https://www.c2es.org/wp-content/uploads/2019/12/cop-25-madrid-summary-1.pdf

[2] Center for Climate and Energy Solutions, Outcomes of the U.N Climate Change Conference in Madrid. Technical Report, Center for Climate and Energy Solutions, 2019.https://www.c2es.org/wp-content/uploads/2019/12/cop-25-madrid-summary-1.pdf

[3] IPCC, Fifth Assessment Report: Summary for Policy Makers. Technical Report, IPCC, 2014.https://www.ipcc.ch/site/assets/uploads/2018/02/WG1AR5_SPM_FINAL.pdf

[4] IPCC, Special Report: Global Warming of 1.5C: Summary for Policymakers. Technical Report, IPCC, 2018.https://www.ipcc.ch/site/assets/uploads/sites/2/2019/05/SR15_SPM_version_report_LR.pdf

[5] Rijksoverheid, Klimaatakkoord. Technical Report, Rijksoverheid, 2019.https://www.klimaatakkoord.nl/binaries/klimaatakkoord/documenten/publicaties/2019/06/28/klimaatakkoord/klimaatakkoord.pdf

[6] W. van Westering, H. Hellendoorn, Low voltage power grid congestion reduction using a community battery: design principles, control and experimental validation, Int. J. Electr. Power Energy Syst. 114 (May 2019) (2020) 105349, https://doi.org/10.1016/j.ijepes.2019.06.007.

[7] P. Staudt, B. Rausch, J. Gärttner, C. Weinhardt, Predicting transmission line congestion in energy systems with a high share of renewables. 2019 IEEE Milan PowerTech, PowerTech 2019, 2019, https://doi.org/10.1109/PTC.2019.8810527.

[8] M.T. Costa-Campi, D. Davi-Arderius, E. Trujillo-Baute, Analysing electricity flows and congestions: looking at locational patterns, Energy Policy 156 (April) (2021) 112351, https://doi.org/10.1016/j.enpol.2021.112351.

[9] I. Bouloumpasis, D. Steen, L.A. Tuan, Congestion management using local flexibility markets: recent development and challenges. Proceedings of 2019 IEEE PES Innovative Smart Grid Technologies Europe, ISGT-Europe 2019, 2019, https://doi.org/10.1109/ISGTEurope.2019.8905489.

[10] C. Kockel, L. Nolting, J. Priesmann, A. Praktiknjo, Does renewable electricity supply match with energy demand?—A spatio-temporal analysis for the German case, Appl. Energy 308 (October 2020) (2022) 118226, https://doi.org/10.1016/j.apenergy.2021.118226.

[11] H.C. Gils, T. Pregger, F. Flachsbarth, M. Jentsch, C. Dierstein, Comparison of spatially and temporally resolved energy system models with a focus on Germany's future power supply, Appl. Energy 255 (September) (2019) 113889, https://doi.org/10.1016/j.apenergy.2019.113889.

[12] RVO, Advanced Scenario Management - Phase 2, 2016, https://www.rvo.nl/subsidies-regelingen/projecten/advanced-scenario-management-phase-2.

[13] Quintel Intelligence, Energy transition model, 2022, https://energytransitionmodel.com/.

[14] Geodan, ASM2 Energy Transition Viewer, 2021, https://pico.geodan.nl/asm2/#/viewer.

[15] Geodan, ASM2 Energy Transition API, 2021, https://pico.geodan.nl/asm2/#/api.

[16] IEA, Wind Power. Technical Report, IEA, Paris, 2021.https://www.iea.org/reports/wind-power

[17] Netbeheer Nederland, Aanbieding integrale infrastructuurverkenning 2030–2050, https://www.rijksoverheid.nl/documenten/brieven/2020/04/02/aanbieding-integrale-infrastructuurverkenning-2030-2050.

[18] DNV-GL, North Sea Energy Outlook. Technical Report, DNV-GL, Arnhem, 2020.

[19] A. Bili, D.G. Vagiona, Use of multicriteria analysis and GIS for selecting sites for onshore wind farms: the case of Andros Island (Greece), Eur. J. Environ. Sci. 8 (1) (2018) 5–13, https://doi.org/10.14712/23361964.2018.2.

[20] C.V. Weiss, P.R.A. Tagliani, J.M.A. Espinoza, L.T. de Lima, T.B.R. Gandra, Spatial planning for wind farms: perspectives of a coastal area in southern Brazil, Clean Technol. Environ. Policy 20 (3) (2018) 655–666, https://doi.org/10.1007/s10098-018-1494-6.

[21] A. Azzellino, C. Lanfredi, L. Riefolo, P. Contestabile, D. Vicinanza, Combined exploitation of offshore wind and wave energy in the Italian seas: a spatial planning approach, Front. Energy Res. 7 (APR) (2019) 1–15, https://doi.org/10.3389/fenrg.2019.00042.

[22] J. Schallenberg-Rodríguez, N. García Montesdeoca, Spatial planning to estimate the offshore wind energy potential in coastal regions and islands. Practical case: the Canary Islands, Energy 143 (2018) 91–103, https://doi.org/10.1016/j.energy.2017.10.084.

[23] Minister van economische zaken en klimaat, Kamerstuk 33561: nummer 42, 2018, https://zoek.officielebekendmakingen.nl/kst-33561-42.html.

[24] Minister van economische zaken en klimaat, Kamerstuk 33561: nummer 48, 2019, https://zoek.officielebekendmakingen.nl/kst-33561-48.html.

[25] Kalavasta, Uitwerking van een 2030 Scenario op Basis van het Ontwerp Klimaatakkoord en vast en Voorgenomen Beleid. Technical Report, Kalavasta, 2019.https://kalavasta.com/assets/reports/Kalavasta2030KEAenergiesysteemNL.pdf

[26] B. den Ouden, J. Kerkhoven, J. Warnaars, R. Terwel, M. Coenen, T. Verboon, T. Tiihonen, A. Koot, Klimaatneutrale Energiescenario's 2050: Scenariostudie ten Behoeve van de Integrale Infrastructuurverkenning 2030–2050. Technical Report, Kalavasta, Berenschot, 2020.https://www.rijksoverheid.nl/documenten/rapporten/2020/03/31/klimaatneutrale-energiescenarios-2050

[27] The Wind Power, Wind turbines [dataset], 2019, https://www.thewindpower.net/store_manufacturer_turbine_en.php?id_type=4.

[28] The Wind Power, Power curves [dataset], 2019, https://www.thewindpower.net/store_manufacturer_turbine_en.php?id_type=7.

[29] Bosch & van Rijn, Windstats statistieken (April 2021) [GIS dataset], 2021, https://windstats.nl/statistieken/.

[30] RVO, SDE(+) projecten in beheer (April 2021) [dataset], 2021, https://www.rvo.nl/sites/default/files/2021/04/SDEplusProjecteninbeheerapril2021.xlsx.

[31] Kadaster, Basisregistratie Adressen en Gebouwen (BAG) [GIS dataset], 2017, https://www.pdok.nl/introductie/-/article/basisregistratie-adressen-en-gebouwen-ba-1.

[32] International Electrotechnical commission, Wind turbines - part 1: design requirements (IEC 61400-1:2005), 3.0 edition, 2005.

[33] G. Geertsema, H. van den Brink, Windkaart van Nederland op 100 m Hoogte, KNMI Publication, 2014.

[34] CBS, Wijk- en buurtkaart [GIS dataset], 2017https://www.cbs.nl/nl-nl/dossier/nederland-regionaal/geografische-data/wijk-en-buurtkaart-2017.

[35] B. de Sonneville, E. Weekamp, P. Rooijmans, H. Hussin, E. Holtsag, Study into Levelized Cost of Energy of Variants for Wind Farm Site Boundaries of Hollandse Kust (West), Ten Noorden van de Waddeneilanden and IJmuiden Ver. Technical Report, Blix Consultancy & Pondera, 2018.

[36] Rijkswaterstaat, Aangewezen windgebieden Netherlands Water Partnership (NWP) [GIS dataset], 2018, https://data.overheid.nl/dataset/49974-aangewezen-windgebieden-nwp#panel-4-downloadable-files.

[37] B.H. Bulder, G. Bedon, E. Bot, Optimal Wind farm Power Density Analysis for Future ofzfshore Wind Farms, ECN Publication, 2018.

[38] D. Sijmons, Energie & Ruimte: een Nationaal Perspectief, Vereniging Deltametropool, Rotterdam, 2017.

[39] Oemof Developer Group, Windpowerlib Documentation. Technical Report, Oemof Developer Group, 2019, https://doi.org/10.5281/zenodo.3403360.

[40] KNMI, Dutch offshore wind atlas: time series files from 2008to 2017 at 10–600 m height at individual 2.5 km grid location [GIS database], 2018, https://data.knmi.nl/datasets/dowa_netcdf_ts_singlepoint/1?q=wind.

[41] E. Hau, Windkraftanlagen: Grundlagen, Technik, Einsatz, wizrschaftlichkeit, 4 ed., 2008.

[42] K. Knorr. Modellierung von raum-zeitlichen Eigenschaften der Windenergieeinspeisung für Wetterdatenbasierte Windleistungssimulationen, Universität Kassel, 2016. Ph.D. thesis.https://kobra.uni-kassel.de/bitstream/handle/123456789/2017020852024/DissertationKasparKnorr.pdf;jsessionid=4F2F5538046EBE15ED39405D4C017443?sequence=7

[43] L. Svenningsen, Power curve air density correction and other power curve options in WindPRO, EMD Int. A/S 1 (2010) 4.

[44] L. Svenningsen, Proposal of an improved power cuve correction, EMD Int. A/S 1 (2010).

[45] M. Biank. Methodology, Implementation and Validation of a Variable Scale Simulation Model for Windpower Based on the Georeferenced Installation Register of Germany, Reiner Lemoine Institute, 2014. Ph.D. thesis.

[46] F. Montealegre, S. Boutsikoudi, Wind Resource assessment and yield prediction: Post Construction analysis. Technical Report, Ecofys, 2014.

[47] CBS, Windenergie: elektriciteitsproductie, capaciteit en windaanbod [dataset], 2019. https://data.overheid.nl/dataset/2294-windenergie–elektriciteitsproductie–capaciteit-en-windaanbod–2002-2019.

[48] I. Maassen van den Brink, N. Olijve, W. Pustjens, Determination of the Cost Levels of Wind Farms (And Their Grid Connections) in New Offshore Wind Energy Search areas. Technical Report, Blix Consultancy & Pondera, 2020.